Geomorphology 105 (2009) 232–238

Contents lists available at ScienceDirect

Geomorphology

journal homepage: www.elsevier.com/locate/geomorph

Deep-seated failure propagation in a fractured rock slope over 10,000 years: The La Clapière slope, the south-eastern French Alps

Samyr El Bedoui [a,*], Yves Guglielmi [a], Thomas Lebourg [a], Jean-Louis Pérez [b]

[a] UMR Géosciences Azur-CNRS-UNS-IRD-UPMC, 250 Avenue Albert Einstein, 06560 Sophia-Antipolis, France
[b] Centre d'Etudes Techniques de l'Equipement Méditerranée-Laboratoire régional de Nice, 56 Bd Stalingrad, 06359 Nice Cedex 4, France

ARTICLE INFO

Article history:
Received 4 April 2008
Received in revised form 2 September 2008
Accepted 26 September 2008
Available online 1 November 2008

Keywords:
Progressive failure
Surface displacements
La Clapière
DGSD

ABSTRACT

The "La Clapière" area (Tinée valley, Alpes Maritimes, France) is a typical large, complex, unstable rock slope affected by Deep Seated Gravitational Slope Deformations (DGSD) with tension cracks, scarps, and a 60×10^6 m^3 rock slide at the slope foot that is currently active. The slope surface displacements since 10 ka were estimated from ^{10}Be ages of slope gravitational features and from morpho-structural analyses. It appears that tensile cracks with a strike perpendicular to the main orientation of the slope were first triggered by the gravitational reactivation of pre-existing tectonic faults in the slope. A progressive shearing of the cracks then occurred until the failure of a large rock mass at the foot of the slope. By comparing apertures, variations and changes in direction between cracks of different ages, three phases of slope surface displacement were identified: 1) an initial slow slope deformation, spreading from the foot to the top, characterized by an average displacement rate of 4 mm yr^{-1}, from 10–5.6 ka BP; 2) an increase in the average displacement rate from 13 to 30 mm yr^{-1} from the foot to the middle of the slope, until 3.6 ka BP; and 3) development of a large failure at the foot of the slope with fast displacement rates exceeding 80 mm yr^{-1} for the last 50 years. The main finding of this study is that such a large fractured slope destabilization had a very slow displacement rate for thousands of years but was followed by a recent acceleration. The results obtained agree with several previous studies, indicating that in-situ monitoring of creep of a fractured rock slope may be useful for predicting the time and place of a rapid failure.

1. Introduction

Mountain slopes are often affected by large, slow and deep-seated deformations with specific morphological features such as counter scarps, double ridges, and trenches (Dramis and Sorriso-Valvo, 1994; Bovis and Evans, 1996; Julian and Anthony, 1996; Agliardi et al., 2001; Kinakin and Stead, 2005). Such deformations lead to progressive movement lasting hundreds to thousands of years (Chigira, 1992; Bovis and Evans, 1996; Crosta and Agliardi, 2002; Brückl and Parotidis, 2005; Jomard, 2006). Studies of the initiation and evolution of deep-seated slope deformations are usually conducted through: (1) laboratory tests on rock samples (Boukharov and Chanda, 1995), (2) physical modelling (Bachmann et al., 2004, 2006), (3) numerical modelling (Agliardi et al., 2001), and (4) field work for landform observations, qualitative mapping and geophysical measurements (Lebourg et al., 2005; Jomard et al., 2007). The laboratory tests usually show a deformation in three phases: (a) a slow initial step with a low and constant deformation rate, (b) an exponential increase of the deformation rate and (c) rupture. Such tests may reproduce natural rock failure evolution over time, but they represent small-scale progressive failure in an initially more or less intact rock sample. Mountain-scale studies of progressive failure rely on physical and numerical studies (Agliardi et al., 2001; Crosta and Agliardi, 2002; Eberhardt et al., 2004; Brückl and Parotidis, 2005; Stead et al., 2006). Bachmann et al. (2004, 2006) proposed slope analogue models with or without persistent large discontinuities. Although they could reproduce typical landforms observed in the field as well as complex deep failure propagation, results remained restricted to homogeneous or only slightly heterogeneous slopes, and changes in processes over time were not considered. Other approaches were based on instrumental monitoring before failure, in an open pit mine (Rose and Hungr, 2007) or a large rock landslide (Crosta and Agliardi, 2003). These studies showed a highly non-linear increase of slip velocity before rock failure that can be expressed by an accelerating creep model. The monitoring, however, was performed over a relatively short time period (several years) whereas we must consider processes lasting several thousand years in the case of deep-seated slope deformations. Moreover, long-term slope processes are complex, which may include a change from an initial slow deformation like creep to a rapid failure.

The study presented here was conducted in a typical alpine mountainous valley, the Tinée, where many active mass movements

* Corresponding author.
E-mail address: bedoui@geoazur.unice.fr (S. El Bedoui).

0169-555X/$ – see front matter © 2008 Elsevier B.V. All rights reserved.
doi:10.1016/j.geomorph.2008.09.025

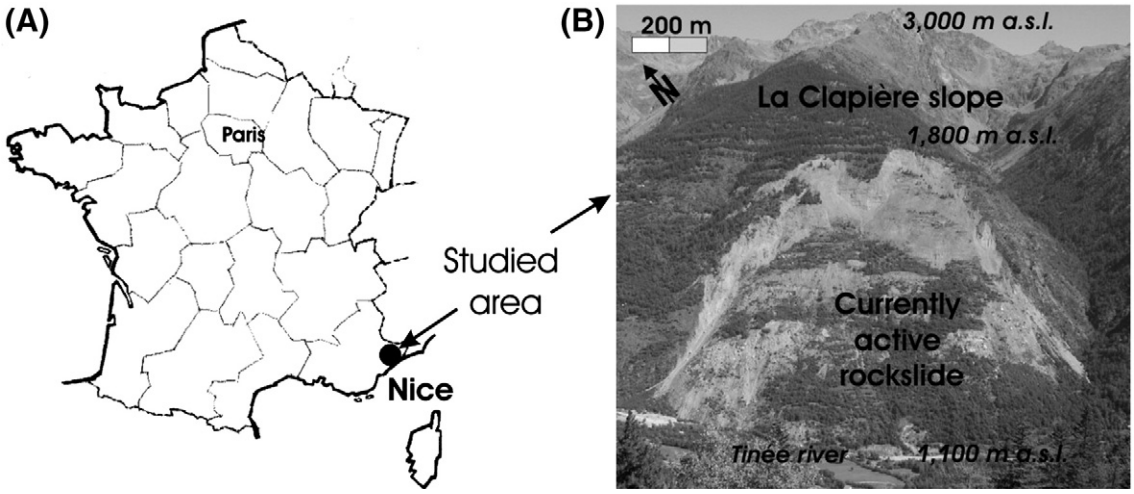

Fig. 1. The study area. A) Location in France. B) Photograph of the La Clapière slope.

occur. A destabilization model for the "La Clapière" rock slope since the last deglaciation (13 ka BP) was constructed from morpho-structural analyses at the slope scale with ^{10}Be dating records used to reconstruct slope deformation with time.

2. Background

The major advances in the research of large-scale slope deformations were achieved by Zischinsky (1966) and Dramis and Sorriso-Valvo (1994). Although such deformations in mountainous landscapes had been regarded as "sackung" (see review in Zischinsky, 1966), they attributed it to creeping of foliated formations, and Dramis and Sorriso-Valvo (1994) called it "Deep Seated Gravitational Slope Deformation" (DGSD). DGSDs have characteristic topographic features including counter scarps, double crests and trenches (Dramis and Sorriso-Valvo, 1994; Agliardi et al., 2001; Kinakin and Stead, 2005). A DGSD mobilizes a large mass with a very slow displacement rate of about several mm yr^{-1} (Bovis and Evans, 1996; Brückl and Parotidis, 2005), whereas earth-flow type landslides usually have a movement rate of several m yr^{-1}. However, slopes affected by DGSDs may induce rapid failure events particularly at the slope foot. The physical and chronological links between these two processes have not been clearly demonstrated (Bovis and Evans, 1996).

To understand slope evolution from DGSD to a rapid failure, it is necessary to underline geometrical links between these two kinds of deformation. This requires conventional field investigations, remote

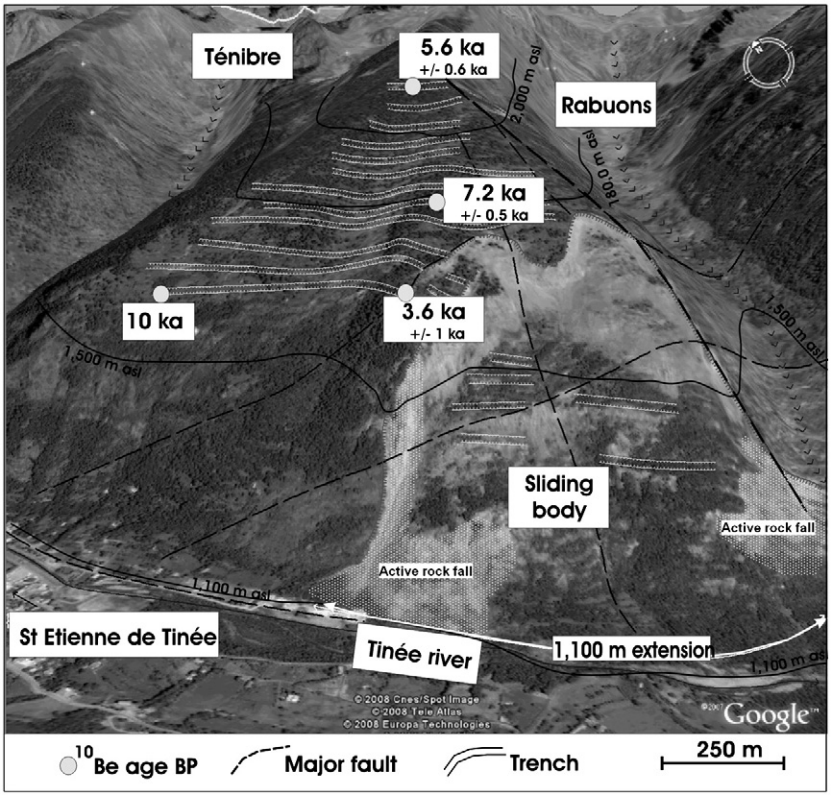

Fig. 2. 3D view of the La Clapière slope. Source: Google Earth.

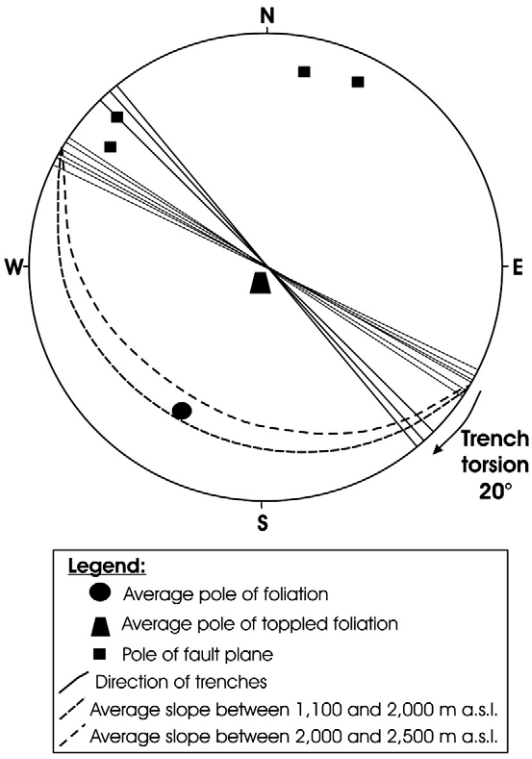

Fig. 3. Stereoplot showing major structural features. (1): major faults; (2): foliation (60°/040°); (3): toppled foliation (005°/040°), (4): trenches (N110° to N140°) and (5) slope direction. The black arrow indicates the trench flexure in the north-western part of the rock slide.

sensing such as air-photo analysis, and the acquisition of relative and absolute chronological constraints over a period of several thousand years. Cosmic ray exposure measurements, in particular ^{10}Be produced in situ, are now widely used to date rock surfaces and fault scarps (Kubik et al., 1998; Bigot-Cormier et al., 2005; Hippolyte et al., 2006), and to estimate erosion rates (Niemi et al., 2005). The method is based on the in-situ production of cosmogenic nuclides (^{10}Be and ^{26}Al) caused by the cosmic ray exposure of surfaces to cosmic rays (Lal, 1991), allowing the exposed surface older than 10 ka BP to be dated with a good accuracy. To apply this method, it is necessary to correct for cosmic ray flux over the exposure time period.

3. The La Clapière slope

The La Clapière slope is located on the north-western side of the Argentera crystalline massif in the southern French Alps (Fig. 1), 80 km upstream from Nice and 1 km downstream from the village of Saint Etienne de Tinée. The slope is bounded by the Tinée river with an orientation of N120° at its foot, and the small Rabuons and Ténibres valleys with an orientation of N000° on its eastern and western sides (Figs. 1B and 2). The slope is 1100 to 3000 m in elevation, and it consists of two sections: (i) a steep section (35°–40°) at the foot to middle slope (up to 2200 m in elevation), and (ii) an upper gentler section with slopes around 25°. This slope morphology is attributed to the Würmian glacial advance and retreat (Julian and Anthony, 1996; Jomard, 2006).

The slope is underlain by the metamorphic hercynian basement including gneiss and migmatite of the Anelle and Iglière units (Bogdanoff and Ploquin, 1980). The Hercynian foliation (mostly 80°/040°) is parallel to the Tinée valley (N120°) but locally toppled (0°/040°, over 80 m thick; Fig. 3). Moreover, the slope is intensely cut at all scales by three families of inherited tectonic structures: N010°–030°, N090°, and N120°–140° (Fig. 3).

From 1960 to 1990, the slope was significantly deformed due to the rock slide activity characterized by a 130-m high scarp in the middle slope. This rock slide activity has been continuously monitored with electronic distance meters and GPS (Géosciences Azur Laboratory) for several years. Currently, the most active part of the rock slide shows a movement of about 0.40 m yr^{-1}, slower than the rate of several m yr^{-1} recorded during the late 1980s. The moving mass has been investigated with structural, mechanical and hydrogeological studies (Follacci, 1987; Ivaldi et al., 1991; INTERREG1, 1996; Cappa and Guglielmi, 2004; Guglielmi et al., 2005), and electrical tomography (Lebourg et al., 2005; Jomard et al., 2007). These studies provided a better understanding of the rock slide, including the geometry of the sliding surface (estimated to be 100 m deep) and links between metoric forcings and slope displacements. Guglielmi et al. (2005) attributed the rock slide to a critical toppling. However, the slope evolution before the rapid deformation has been less well documented.

4. Analysis and evolution of the La Clapière slope

4.1. Topographic analysis

The slope shows signs of large deformation: (i) counter scarps with an off-set of several meters in the upper slope above 2200 m in elevation, and (ii), trenches expressing a traction opening of pre-existing discontinuities in the lower slope (Fig. 4). These morpho-structures are also found in surrounding areas on the left side of the valley affected by DGSDs, from the La Clapière slope to Isola Village (12 km downstream) (Jomard, 2006).

The current deformation at the La Clapière slope extends from the slope toe to 1800 m elevation and affects a rock volume of 60×10^6 m^3 (Fig. 2). Field investigations show that the active rock slide is embedded in the remaining middle and upper parts of the slope which, although currently inactive, display trench-like deformation features extending widely towards the slope crest (Fig. 4). Fifteen trenches with an average orientation of N120° and lengths of 100 to 5000 m were mapped (Fig. 2). In general, trenches occur in major pre-existing fault zones, explaining why the density of these morpho-structures strongly depends on the angular relation between slope direction, foliation and fault orientations. They are much more developed when this angle is close to zero. In other words, the landscape and the structural framework are significantly controlled by the N120° orientation (Fig. 3).

The aperture and the vertical off-set normal to the trench plane were measured at different locations in each trench. The mean horizontal aperture is 1 to 5.5 m (Table 1) and there is no significant

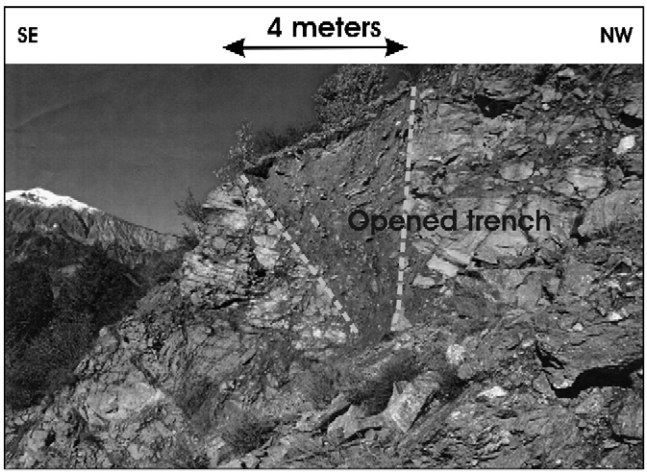

Fig. 4. A trench on the La Clapière slope.

Table 1
Trench aperture measurements

No. of trench (Fig. 5)	1	2	3	4	5	6	7	8	9	10	11	12	13	14	15
Horizontal opening (in m)	3.9	2.8	2.6	2.8	4.2	2.7	1.0	4.3	1.2	3.0	1.3	6.5	2.8	1.7	6.5

lateral variation of the aperture within a single trench. The vertical offset is as small as a few tens of cm in all cases.

Where the average trench orientation is parallel to the slope direction, the orientation turns to N150° near the west boundary of the currently active landslide (Figs. 2, 3 and 5C). Trenches 1 to 4, which are the closest to the landslide scarp, are highly twisted and even cut by the scarp, while torsion becomes moderate in trenches 5 and 6 and non-existent in trenches 7 to 15.

4.2. Chronology of slope deformations

The opening of trenches 1, 6 and 14 and the west lateral scarp propagation of the La Clapière active rock slide were dated with ^{10}Be (for details see Bigot-Cormier et al., 2005). For each structure four samples were measured, and production rates were estimated after the latitudinal and elevation correction, while any geomagnetic variations were retained. ^{10}Be ages and their accuracy are shown in Fig. 2.

Trenches are progressively younger from #1 (10 ka BP), #6 (7.2 ka BP) to #15 (5.6 ka BP), meaning that there was a propagation of slope deformation from the toe to the top in about 4400 years. The upper lateral scarp of the currently active landslide was dated at 3.6 ka BP, showing that after the upslope propagation of the deformation, a deep fault occurred in the middle part of the slope and bounded the currently active landslide. In the landslide body, larger and older trench structures are intensely cut by another active N050° fault plane.

4.3. Conceptual model of progressive failure of the La Clapière slope

From 10 to 5.6 ka BP (Fig. 5A,B), extensional structures (trenches) spread from the toe to the top of the slope (phase I). Although this might be explained as the reactivation of inherited structures induced by the stress-release from the last deglaciation, the earliest deformation dated does not very well match the glacier retreat in the La Clapière area. Previous work (Bigot-Cormier et al., 2005) shows that the Tinée valley and the Rabuons valley were totally deglaciated around 13 ka BP, indicating that the deglaciation was not the direct factor triggering the La Clapière rock slide. Failures in the traction of pre-existing vertical faults predominated, characterized by large horizontal openings of the trenches along an N120° direction.

From 5 to 3.6 ka BP (Fig. 5C), the trenches in the lower eastern part of the slope became twisted and displayed a large vertical displacement (phase II). This three-dimensional deformation related to shearing deep in the slope could be induced by preferential tangential movements along a major reactivated vertical fault zone (N120°) in the eastern part of the slope.

Another failure began in the lower eastern part of the slope at about 3.6 ka BP (Fig. 5C), and during the last 50 years this failure has enlarged and bounded the currently active La Clapière landslide (phase III, Fig. 5D). The current slope deformation is large and diffused, and regressive from 1600 to 2200 m in elevation. It is mainly characterized by horizontal displacement along the slope, and mainly localized in the basal slope. It also includes displacements with a vertical component related to a deep failure surface.

5. Quantification of slope displacement over the last 10,000 years

The conceptual slope failure model relates trench openings in the past to the current La Clapière landslide at the slope toe. Trench morphology can be a good indicator of surface slope deformation at the mountainous scale and for a long period of several thousand years. In this section the proposed approach is quantitatively developed by combining the morphostructural measurements of trenches with the ^{10}Be datings.

5.1. Estimation of average surface velocity in phase I (Fig. 6A)

Surface velocity was calculated using the following equation:

$$V = D/T \quad (1)$$

where V is the velocity (m yr^{-1}), D is the mean surface displacement (m) and T is the time (yr).

The time T was calibrated with the ^{10}Be dates. Trench apertures measured in the field (Table 1) were used to estimate D. Since all trenches have similar lengths and apertures, we hypothesized that, after a critical maximum opening, the trench did not evolve, and the deformation with a new trench opening propagated towards the upper part of the slope. If we consider that all trenches located between two dated points opened during the time period between the two dates and did not significantly evolve afterwards, average D can be estimated from the apertures of the trenches (Fig. 6A). Based on this assumption, D and V for the period between 10 and 7.2 ka BP and between 7.2 and 5.6 ka BP were estimated, using a longitudinal section along the western part of the slope (Fig. 5D) which is not significantly affected by the current La Clapière landslide evolution (Fig. 6A). In our estimation of D, the basal part of the slope is considered fixed, because no major trench-like deformations were mapped in that area. The accuracy of this velocity estimation relies on the ^{10}Be ages accuracy (Bigot-Cormier et al., 2005) and on the error of field measurements of trench apertures. The latter was considered to be ±1 m based on the σ value of the 15 aperture measurements in Table 1.

The results show that between 10.3 and 7.2 ka, the total opening of the trenches (D) was about 19 m. The corresponding average V is 6.1 ± 2.9 mm yr^{-1}. Between 7.2 and 5.6 ka BP, the total opening of the trenches was 25 m, and the corresponding average V is 15.2 ± 4.8 mm yr^{-1}.

5.2. Estimation of surface velocity in phase II (Fig. 6B)

Phase II is characterized by twisting of trenches 1 to 6 until the initiation of the current La Clapière landslide scarp at 3.6 ka BP. Measurements from trench 1 were used to estimate the phase II surface velocity. An accurate levelling of the trench was performed with a spacing of 50 m. Points located in the western part of the trench that were not affected by phase II deformation were used to estimate the direction of the trench before phase II, using a linear regression algorithm (Fig. 3). Average displacement D was estimated by comparing the location of the other points with the pre-phase II trench direction. The resulting D is 26 ± 5.0 mm yr^{-1} for the period 5.6 to 3.6 ka BP.

5.3. Temporal variation of surface deformation velocity (Fig. 7)

There has been a non-linear increase of surface deformation velocity since 10 ka. The oldest dated deformations of the La Clapière slope are extensional trench-like structures that evolved from the foot to the top of the slope (phase I, Fig. 5A,B) with velocity increasing from 6 to 15 mm yr^{-1}. At 3.6 ka BP, a localization of shear deformations occurred in the south-eastern part of the slope (Fig. 5C) that induced a

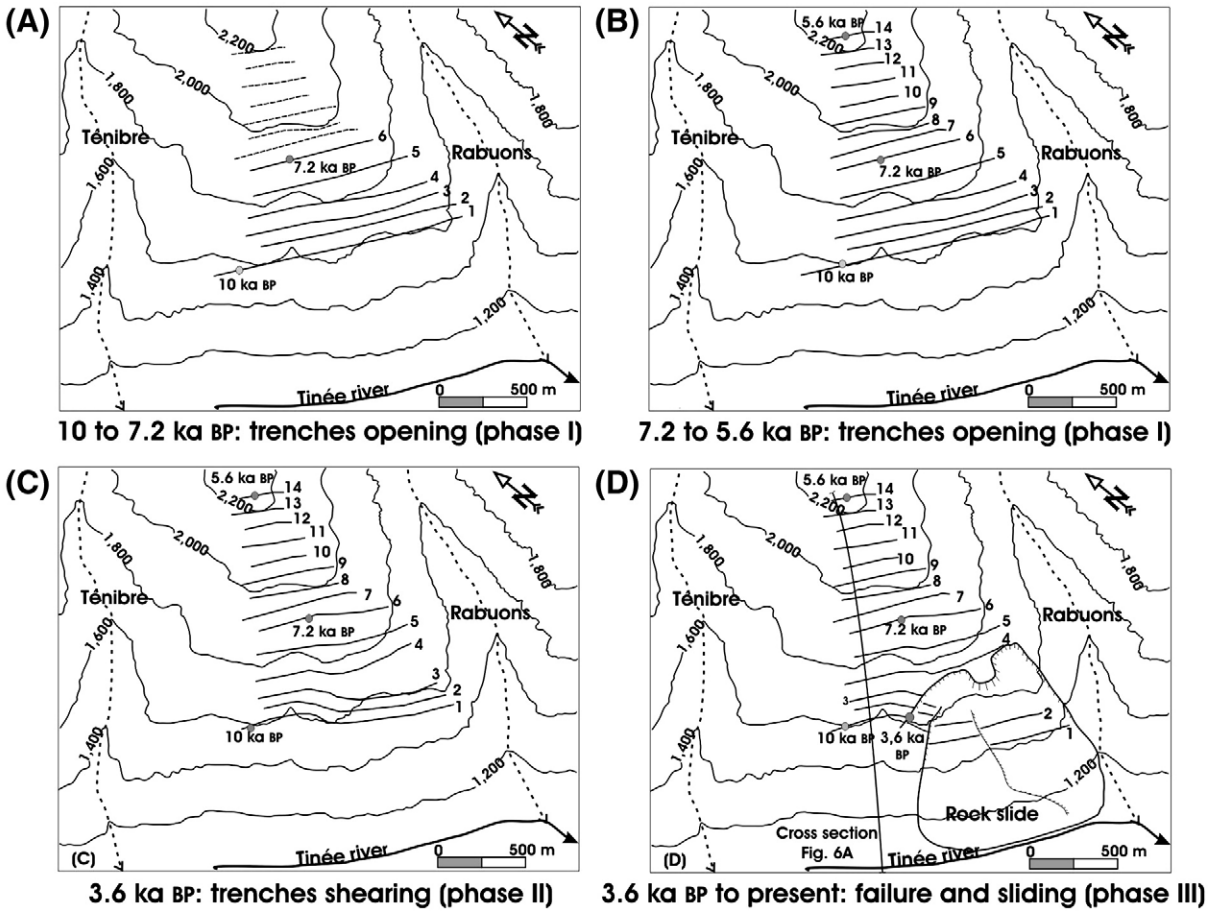

Fig. 5. Evolution of the La Clapière slope deformation for the last 10,000 years. (A): trench opening at 10 to 7.2 ka BP from 1600 to 2250 masl; (B) that at 7.2 to 5.6 ka BP; (C) surface shearing close to the future rock slide area at 3.6 ka BP; (D) rock slide collapse and sliding since 3.6 ka BP.

local twisting of trenches at velocities of 15 to 40 mm yr^{-1}, while the remaining part of the slope was stabilizing. Finally, in 1960, the current La Clapière landslide was triggered (phase III, Fig. 5D) moving at velocities of 80 to 1000 mm yr^{-1}.

6. Discussion

6.1. Accuracy of the estimated slope surface deformation velocities

The velocity *V* for phase I was very low and its variation between 10 and 7.2 ka BP and 7.2 to 5.6 ka BP depends on the accuracy of the age estimations (Fig. 7). Modelling has also shown that the slope toe can be affected by blind gravitational faults hidden by alluvial deposits along a valley (Hippolyte et al., 2006). Therefore, our method gives only a rough estimation of the average slope displacement.

The velocity *V* for phase II showed a significant increase to 30 mm yr^{-1} (Fig. 7). Nevertheless, this velocity change is calculated using only two dated morphologies of a single trench: 10 ka BP (trench opening) and 3.6 ka BP (trench cutting by surface failure propagation). This estimation eventually assumes that the trench twisting started immediately after the trench opening and continued until 3.6 ka BP. There may have been variations in velocity of short duration.

The velocity *V* for phase III (since 3.6 ka) is 80 mm yr^{-1} on average (Fig. 7). Monitoring over 30 years shows a marked oscillation of landslide velocity with several peaks of up to 1000 mm yr^{-1} and periods of much slower movement. The acceleration of the movement more clearly occurred during the last 10 years, whereas the mean *V* for the period from 3.6 ka BP to 1960 was close to that for phase II. In addition, spatial variations in velocity depending on the location of the measuring points are clearly observed within the sliding body, indicating the behaviour of a highly heterogeneous fractured rock mass (Follacci, 1987), which confirms that our approach only provides a rough reconstruction of progressive slope failure.

6.2. Linking surface deformation to deep progressive failure processes

The mountain-scale extension of the observed surface deformations involves gravitational processes deep in the slope. Previous studies (Eberhardt et al., 2004; Bachmann et al., 2006; Stead et al., 2006) proposed complex models where the slope was affected by large unconnected vertical faults separating deep intact areas. The failure developed slowly from the foot to the top, explaining the extensive occurrence at the surface of morphostructural features (trenches, counters scarps, and double ridges).

To explain the kinematics of the mobile part with local trenches, a failure at least 200 m deep must be considered (Lebourg et al., 2005). Before the rock slide was triggered, the slope was cut by two families of inherited discontinuities (represented by the N020°- and N090°-oriented faults) which bound its eastern and upper sections, respectively. Several discontinuities were then generated during the formation of the trenches. Conversely, the current western boundary of the rock slide was not pre-cut by any inherited discontinuity. During the slow evolution of the slope (phase I and the beginning of phase II), the internal rock mass damage did not affect the western area.

The transition between phases II and III was associated with a large failure of 60×10^6 m^3 and an associated increase of the mean velocity. After that, the differential evolution between the mobile part and the stable western part was distinct and the trench-type deformation at

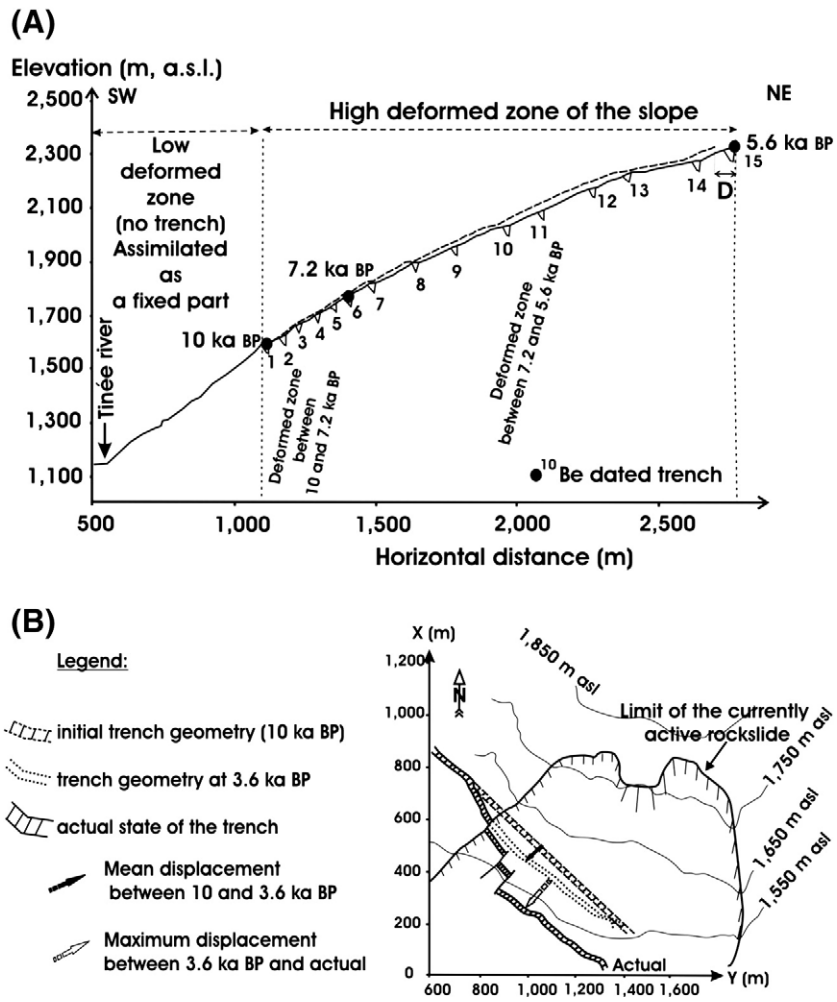

Fig. 6. Methodology to reconstruct paleo-slope geometry. (A) Longitudinal slope section oriented SW-NE. The location of the cross-section is shown in Fig. 5D. Black line: actual topography; dashed line: reconstructed topography after closing of trenches. *D*: relative displacement for the period from 10 to 5.2 ka BP. (B) Reconstitution of the progressive surface shearing since 3.6 ka BP.

the surface ceased. This may indicate that major discontinuities and their geometrical configuration played a key role during phase III in determining the location of the rapid event, although during phases I and II, slope creep seems to have been more controlled by the general slope form and rock strength parameters at the slope scale.

6.3. Time before failure at large and small time scales

The model of slope-surface morphological evolution proposed here largely matches laboratory experiments which clearly show non-linear creep processes even for hard rocks. Creep evolution is considered to be composed of three phases (Boukharov and Chanda, 1995): the primary and secondary creeping phases characterized by a linear strain–time relation, and the tertiary creeping phase with an exponentially increasing velocity prior to failure. This evolution, and especially the tertiary phase, can be mechanically explained from progressive localized failure due to a stress concentration.

Brückl and Parotidis (2005) numerically studied slope instabilities due to deep-seated gravitational creep (DSGC) and discussed the transition between a slow creeping phase and a rapid sliding. The slow creeping episode corresponds to phases I and II, while rapid sliding occurs in phase III described in this study. Brückl and Parotidis (2005)

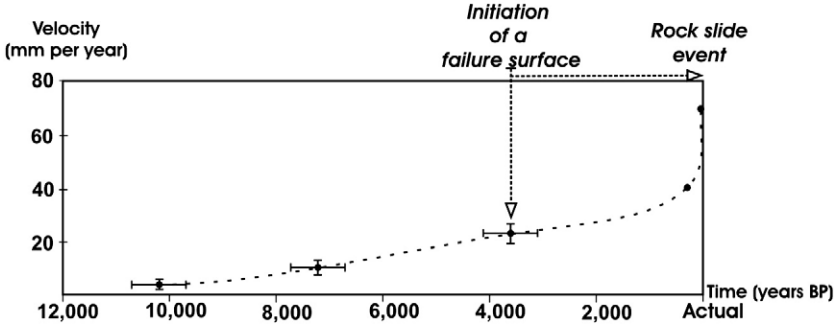

Fig. 7. La Clapière slope velocity for the last 10 ka.

estimated that the primary phases in the Austrian Alps occurred from 13 to 5.5 ka BP with velocities of 5 to 8 mm yr^{-1}, which agrees well with our velocity estimates.

Other studies on slope deformation velocity before failure, based on numerical modelling and instrumental surveys (Crosta and Agliardi, 2002, 2003; Petley et al., 2005; Rose and Hungr, 2007), describe slow and a constant displacement velocity (a few ten of m yr^{-1}) before an exponential increase in velocity soon before failure (around 10 m yr^{-1}). Although these studies considered only a short time period (several months), such velocity values match the results presented here for phases I and II.

In view of the agreement between the results of our work and that of previous studies of slopes sliding under different geological and structural conditions, we conclude that long-term deformation of the slope is more related to complex rheology than to the slope heterogeneity. Numerical modelling is needed to explore the geomechanical processes involved and the role of first-order heterogeneities such as major faults in the processes involved but this is beyond the scope of the present paper. In particular, it appears necessary to consider roles and effects of rock strength parameters on the slope evolution.

7. Conclusion

Combining a chronological study with geomorphological mapping, we have shown that slope evolution from a large-scale deformation (DGSD) to a rapid failure can be regarded as the evolution of creep that leads to faster and more localized displacements. We have identified three phases of slope evolution: I) a slow large-scale deformation (4 mm yr^{-1}) with opening of trenches, over a long time period (10 ka to 5.6 ka BP); II): a localized deformation with faster displacement (13 to 30 mm yr^{-1}) in a shorter period (3.6 ka BP); and III) a rapid failure at the slope foot in a short time period (50 years), with a very high displacement rate (>80 mm yr^{-1}). The result presented here agrees with several previous studies, which indicates that instrumental surveys (e.g., GPS) of creeping of slopes affected by DGSD may enable the estimation of the time of a future rapid failure.

Acknowledgements

The authors thank the two anonymous reviewers and the Editor for their very constructive comments which greatly improved the manuscript. We thank Pr Guust Nolet for his comments and English corrections.

References

Agliardi, F., Crosta, G., Zanchi, A., 2001. Structural constraints on deep seated slope deformation kinematics. Engineering Geology 59, 83–102.
Bachmann, D., Bouissou, S., Chemenda, A., 2004. Influence of weathering and pre-existing large scale fractures on gravitational slope failure: insights from 3-D physical modelling. Natural Hazards and Earth Sciences 4, 711–717.
Bachmann, D., Bouissou, S., Chemenda, A., 2006. Influence of large scale topography on gravitational rock mass movements: new insights from physical modelling. Geophysical Research 33, 1–4.
Bigot-Cormier, F., Braucher, R., Bourlès, D., Guglielmi, Y., Dubar, M., Stéphan, J.-F., 2005. Chronological constraints on processes leading to large active landslides. Earth and Planetary Science Letters 235, 141–150.
Bogdanoff, S., Ploquin, A., 1980. Les gneiss et migmatites du Massif de l'Argentera (Alpes-Maritimes): apport de deux coupes géochimiques. Bulletin de la Société Géologique de France XXII (no 3), 353–358.
Boukharov, G.N., Chanda, M.W., 1995. The three processes of brittle crystalline rock creep. International Journal of Rock Mechanics and Mining Science 32, 325–335.
Bovis, M.J., Evans, S.G., 1996. Extensive deformations of rock slopes in southern Coast Mountains, southwest British Columbia, Canada. Engineering Geology 44, 163–182.
Brückl, E., Parotidis, M., 2005. Prediction of slope instabilities due to deep-seated gravitational creep. Natural Hazards and Earth System Sciences 5, 155–172.
Cappa, F., Guglielmi, Y., 2004. Hydromechanical modelling of a large moving rock slope inferred from slope levelling coupled to spring long-term hydrochemical monitoring: example of the "La Clapière" landslide (Southern Alps, France). Journal of Hydrogeology 291, 67–90.
Chigira, M., 1992. Long-term gravitational deformation of rocks by mass rock creep. Engineering Geology 32, 157-154.
Crosta, G.B., Agliardi, F., 2002. How to obtain alert velocity thresholds for large rock slides. Physics and Chemistry on the Earth 27, 1557–1565.
Crosta, G.B., Agliardi, F., 2003. Failure forecast for large rock slides by surface displacement measurements. Canadian Geotechnical Journal 40, 176–191.
Dramis, F., Sorriso-Valvo, M., 1994. Deep-seated gravitational slope deformations, related landslides and tectonics. Engineering Geology 38, 231–243.
Eberhardt, E., Stead, D., Coggan, J.S., 2004. Numerical analysis of initiation and progressive failure in natural rock slopes — the 1991 Randa rock slide. International Journal of Rock Mechanics and Mining Science 41, 69–87.
Follacci, J.P., 1987. Les mouvements du versant de La Clapière à Saint Etienne de Tinée (Alpes Maritimes). Bulletin du Laboratoire des Ponts et Chaussées 150–151, 39–54.
Guglielmi, Y., Cappa, F., Binet, S., 2005. Coupling between hydrogeology and deformation of mountainous rock slopes: insights from La Clapière area (southern Alps, France). Comptes Rendus Géosciences 337, 1154–1163.
Hippolyte, J.C., Brocard, G., Tardy, M., Nicoud, G., Bourlés, D., Braucher, R., Ménard, G., Souffaché, B., 2006. The recent fault scarps of the Western Alps (France): tectonic surface ruptures or gravitational sackung scarps? A combined mapping, geomorphic, levelling, and ^{10}Be dating approach. Tectonophysics 418, 255–276.
INTERRREG1, 1996. Risques générés par les grands mouvements de versant, étude comparative de 4 sites des Alpes franco-italiennes. Programme INTERREG 1, France — Italie, Regione Piemonte-University J. Fourier, LIRIGM Grenoble, p. 207.
Ivaldi, J.P., Guardia, P., Follacci, J.P., Terramorsi, S., 1991. Plis de couverture en échelons et failles de second ordre associés à un décrochement dextre de socle sur le bord nord-ouest de l'Argentera (Alpes-Maritimes, France). Compte Rendus de l'Académie des Sciences Paris 313 (II), 361–368.
Jomard, H., 2006. Analyse multi-échelles des deformations gravitaires du Massif de l'Argentera Mercantour. PhD Thesis, University Nice Sophia Antipolis, 246 pp.
Jomard, H., Lebourg, T., Tric, E., 2007. Identification of the gravitational boundary in weathered gneiss by geophysical survey: La Clapière landslide (France). Journal of Applied Geophysics 62, 47–57.
Julian, M., Anthony, E., 1996. Aspects of landslide activity in the Mercantour Massif and the French Riviera, southeastern France. Geomorphology 15, 275–289.
Kinakin, D., Stead, D., 2005. Analysis of the distributions of stress in natural ridges forms: implications for the deformation mechanisms of rock slopes and the formation of sacking. Geomorphology 65, 85–100.
Kubik, P.W., Ivy-Ochs, S., Masarik, J., Frank, M., Schlüchter, C., 1998. ^{10}Be and ^{26}Al production rates deduced from an instantaneous event within the dendrocalibration curve, the landslide of Köfels, Ötz Valley, Austria. Earth and Planetary Science Letters 161, 231–241.
Lal, D., 1991. Cosmic ray labelling of erosion surfaces: in situ nuclide production rates and erosion models. Earth and Planetary Science Letters 104, 424–439.
Lebourg, T., Binet, S., Tric, E., Jomard, H., El Bedoui, S., 2005. Geophysical survey to estimate the 3D sliding surface and the 4D evolution of the water pressure on part of a deep seated landslide. Terra Nova 17, 399–406.
Niemi, N.A., Oskin, M., Burbank, D.W., Heimstah, A.M., Gabet, E.J., 2005. Effects of bedrock landslides on cosmogenically determined erosion rates. Earth and Planetary Sciences Letters 237, 480–498.
Petley, D.N., Mantovani, F., Bulmer, M.H., Zannoni, A., 2005. The use of surface monitoring data for the interpretation of landslide movement patterns. Geomorphology 66, 133–147.
Rose, N.D., Hungr, O., 2007. Forecasting potential rock slope failure in open pit mines using the inverse-velocity method. Technical note. Rock Mechanics and Mechanics and Mining Sciences 44, 308–320.
Stead, D., Eberhardt, E., Coggan, J.S., 2006. Developments in the characterization of complex rock slope deformation and failure using numerical modelling techniques. Engineering Geology 83, 217–235.
Zischinsky, U., 1966. On the Deformation of High Slopes. Proc. 1st Conference International of the Society of Rock Mechanics, Lisbon, 2, pp. 179–185.